# Bosonic Andreev bound state

Nobuyuki Okuma [*]

*Graduate School of Engineering, Kyushu Institute of Technology, Kitakyushu 804-8550, Japan*

(Received 20 October 2023; revised 26 June 2024; accepted 8 July 2024; published 23 July 2024)

A general free bosonic system with a pairing term is described by a bosonic Bogoliubov-de Gennes (BdG) Hamiltonian. The representation is given by a pseudo-Hermitian matrix, which is crucially different from the Hermitian representation of a fermionic BdG Hamiltonian. In fermionic BdG systems, a topological invariant of the whole particle (hole) bands can be nontrivial, which characterizes the Andreev bound states (ABS), including Majorana fermions. In bosonic cases, on the other hand, the corresponding topological invariant is thought to be trivial, owing to the stability condition of the bosonic ground state. In this paper, we consider a two-dimensional model that realizes a bosonic analogy of the ABS at the boundaries. The boundary states of this model are located outside the bulk bands and are characterized by a nontrivial Berry phase (or polarization) of the hole band. Furthermore, we investigate the zero-energy flat-band limit in which the Bloch Hamiltonian is defective, where the particle and hole states are identical to each other. In this limit, the Berry phase is $\mathbb{Z}_2$ quantized thanks to an emergent parity-time symmetry induced by the defective nature. This is an example of a topological invariant that uses the defective nature as a projection structure. Thus, boundary states in our model are essentially different from Hermitian topological modes and their variants. We also discuss the entanglement entropy of the system with bosonic Andreev bound states, motivated by the relationship between our model and the continuous variable surface codes.

DOI: 10.1103/PhysRevB.110.014516

## I. INTRODUCTION

The bosonic excitations from a Bose-Einstein condensate are well described by a quadratic Hamiltonian called the bosonic Bogoliubov-de Gennes (BdG) Hamiltonian [1–4]. As well as the systems that consist of bosons such as photons [5,6] and bosonic atoms [3], the bosonic BdG Hamiltonian can describe emergent bosonic quasiparticles in ordered states such as magnons [7] and phonons [8]. Unlike the fermionic counterpart, its excitation spectrum is related to the eigenspectrum of a pseudo-Hermitian Hamiltonian matrix with a particle-hole symmetry [9] if there exists a paring term, which breaks the particle-number conservation. This is an example of the non-Hermitian system whose non-Hermiticity originates not from an open quantum nature but from the linear approximation of a nonlinear equation.

Recently, a lot of concepts in topological physics [10,11] have been generalized to bosonic BdG Hamiltonians even though the representation matrix is pseudo-Hermitian [7]. For example, the Chern number is defined by using a paraunitary matrix, and it characterizes the bulk-boundary correspondence [12] as in the case of Hermitian topological physics [13]. Similar generalizations for other topological numbers such as the $\mathbb{Z}_2$ invariant have been extensively studied [14]. In the language of non-Hermitian topological physics [15–17], this is a manifestation of the line-gap topology, which is adiabatically connected to the Hermitian topology without closing the gap and changing the symmetry [18].

One interesting direction is to seek topological boundary states that reflect the BdG nature. In fermionic cases, a topological number of the whole particle (hole) bands can be nontrivial, and it describes the Andreev bound states (ABS) including Majorana fermions [19,20]. In bosonic cases, on the other hand, the corresponding topological invariant can not be nontrivial if we limit our discussion to a topological phase transition in Kitaev's periodic table [21,22], which requires a nontrivial band inversion process. For the stability of the ground state, the bosonic excitation energies should be nonnegative. Owing to this stability condition, the BdG Hamiltonian is adiabatically connected to a trivial Hamiltonian without closing the gap between the particle and hole bands [12].

In this paper, we investigate a BdG Hamiltonian on the two-dimensional square lattice and find a bosonic analogy of ABS at the boundaries that are induced by a nontrivial Berry phase of the particle (hole) bands defined in an unconventional manner. In an extreme limit, the Berry phase is $\mathbb{Z}_2$ quantized, owing to an emergent parity-time symmetry. This quantization can be understood as the non-Hermitian topology that uses the defective nature as a projection structure. We also discuss the entanglement entropy of our model, motivated by the similarity with continuous variable surface codes.

This paper is organized as follows. In Sec. II, we review the basics of the free bosonic BdG Hamiltonian and introduce notations in this paper. In particular, we focus on the non-Hermitian nature of the bosonic BdG Hamiltonian. In Sec. III, we define a model with bosonic boundary states, which are characterized by the nontrivial Berry phase defined in an unconventional manner. In Sec. IV, we consider the

[*]Contact author: okuma@hosi.phys.s.u-tokyo.ac.jp

 

zero-energy flat-band limit in which the Hamiltonian is defective. In this limit, we define the $\mathbb{Z}_2$ topological number protected by the effective parity-time symmetry and the $\mathbb{Z}$ topological number for non-Hermitian defective structure. In Sec. V, we discuss the entanglement structure of the system with bosonic Andreev bound states. In continuous variable surface codes, there exist boundary states similar to our model. Motivated by this similarity, we investigate the topological entanglement entropy of our model.

## II. BASICS OF BOSONIC BDG HAMILTONIAN

First, we review the basic properties of BdG Hamiltonians and define some notations. A translation-invariant lattice BdG Hamiltonian with $N$ internal degrees of freedom is given by [12]

$$\hat{H} = \frac{1}{2}\sum_{\boldsymbol{k}}(\boldsymbol{a}_{\boldsymbol{k}}^\dagger, \boldsymbol{a}_{-\boldsymbol{k}})H_{\boldsymbol{k}}\begin{pmatrix}\boldsymbol{a}_{\boldsymbol{k}} \\ \boldsymbol{a}_{-\boldsymbol{k}}^\dagger\end{pmatrix}, \tag{1}$$

where $\boldsymbol{a}_{\boldsymbol{k}}^\dagger = (a_{1,\boldsymbol{k}}^\dagger, \cdots, a_{N,\boldsymbol{k}}^\dagger)$ denote creation operators of bosons with crystal momentum $\boldsymbol{k}$. $H_{\boldsymbol{k}}$ is a $2N \times 2N$ Hermitian matrix with the following form [12]:

$$H_{\boldsymbol{k}} = \begin{pmatrix} h_{\boldsymbol{k}} & s_{\boldsymbol{k}} \\ s_{-\boldsymbol{k}}^* & h_{-\boldsymbol{k}}^* \end{pmatrix}, \tag{2}$$

where $h_{\boldsymbol{k}}$ and $s_{\boldsymbol{k}}$ are $N \times N$ matrices that represent the normal term and pairing term (anomalous term), respectively. Due to the Hermiticity of $H$, $h$ and $s$ are Hermitian and symmetric matrices, respectively. It is well known that the excitation spectrum of the bosonic BdG Hamiltonian is not given by the eigenspectrum of $H_{\boldsymbol{k}}$ if the pairing term is nonzero, unlike in the case of fermions [1–4]. This is because unitary transformation for the bosonic Nambu spinor destroys the bosonic commutation relation under the pairing term. Thus, the naive unitary diagonalization does not work for the bosonic BdG Hamiltonian. Interestingly, the true excitation spectrum is related to the eigenspectrum of a pseudo-Hermitian matrix with a particle-hole symmetry [9]:

$$H_{\boldsymbol{k}}^\sigma := \sigma_z H_{\boldsymbol{k}}, \tag{3}$$

$$\sigma_z\left[H_{\boldsymbol{k}}^\sigma\right]^\dagger\sigma_z = H_{\boldsymbol{k}}^\sigma, \tag{4}$$

$$\sigma_x\left[H_{-\boldsymbol{k}}^\sigma\right]^*\sigma_x = -H_{\boldsymbol{k}}^\sigma, \tag{5}$$

where $\sigma$'s denote the Pauli matrices in Nambu space. This pseudo-Hermitian matrix is diagonalized by a paraunitary matrix $P_{\boldsymbol{k}}$ [12]:

$$P_{\boldsymbol{k}}^{-1}H_{\boldsymbol{k}}^\sigma P_{\boldsymbol{k}} = \begin{pmatrix} E_{\boldsymbol{k}} & 0 \\ 0 & -E_{-\boldsymbol{k}} \end{pmatrix}, \tag{6}$$

$$P_{\boldsymbol{k}}\sigma_z P_{\boldsymbol{k}}^\dagger = P_{\boldsymbol{k}}^\dagger\sigma_z P_{\boldsymbol{k}} = \sigma_z. \tag{7}$$

Here, $E_{\boldsymbol{k}}$ is the diagonal matrix whose elements $\{\epsilon_{\boldsymbol{k},a} \mid a = 1, \cdots, N\}$ are the excitation energies. An explicit construction of the paraunitary matrix $P$ is given in the Appendix. Note that the excitation energies can be negative or complex without further assumptions. Since the former/latter leads to the Landau/dynamical instability of the ground state [3], the positive semidefiniteness of the Hermitian matrix $H_{\boldsymbol{k}}$ is assumed to realize the nonnegative excitation energies in conventional condensed matter physics [23]. In the following, we call $\{\epsilon_{\boldsymbol{k},a}\}$ and $\{\epsilon_{\boldsymbol{k},-a} := -\epsilon_{-\boldsymbol{k},a}\}$ the particle and hole bands, respectively. Owing to the non-Hermiticity (nonnormality), the bra (left) eigenvectors are not always the hermitian conjugate of the ket (right) eigenvectors:

$$\begin{aligned} \langle\langle \boldsymbol{k}, i|H_{\boldsymbol{k}}^\sigma &= \epsilon_{\boldsymbol{k},i}\langle\langle \boldsymbol{k}, i|, \\ H_{\boldsymbol{k}}^\sigma\,|\boldsymbol{k}, i\rangle &= \epsilon_{\boldsymbol{k},i}\,|\boldsymbol{k}, i\rangle\,, \end{aligned} \tag{8}$$

where $i$ takes both $a$ and $-a$. If we take the biorthonormal convention, the bra and ket eigenvectors are in the following relations [18,24]:

$$|\boldsymbol{k}, i\rangle\rangle = \mathrm{sgn}(i)\sigma_z|\boldsymbol{k}, i\rangle, \tag{9}$$

$$\langle\langle \boldsymbol{k}, i|\boldsymbol{k}, j\rangle = \mathrm{sgn}(i)\,\langle \boldsymbol{k}, i|\,\sigma_z|\boldsymbol{k}, j\rangle = \delta_{i,j}. \tag{10}$$

In topological physics of bosonic BdG systems, the topological invariants are usually defined by using both the right and left eigenvectors. For example, the Berry connection defined in Refs. [12,24,25] is rewritten as follows:

$$\begin{aligned} A_{i,\nu}^{LR}(\boldsymbol{k}) :&= i\mathrm{Tr}[\Gamma_i\sigma_z P_{\boldsymbol{k}}^\dagger\sigma_z(\partial_{k_\nu}P_{\boldsymbol{k}})] \\ &= i\mathrm{Tr}\left[\Gamma_i P_{\boldsymbol{k}}^{-1}(\partial_{k_\nu}P_{\boldsymbol{k}})\right] \\ &= i\langle\langle \boldsymbol{k}, i|\partial_{k_\nu}\,|\boldsymbol{k}, i\rangle\,, \end{aligned} \tag{11}$$

where $\Gamma_i$ is a diagonal matrix taking $+1$ for the $i$th diagonal component and zero otherwise. We have used the paraunitary condition (7) and assumed the biorthonormal convention. The Chern number is defined by using $A_{i,\nu}^{LR}$, which describes the topological physics of the bulk-boundary correspondence. As mentioned in the introduction, these topological invariants cannot be nontrivial for the whole particle (hole) bands if we assume the positive definiteness of $H_{\boldsymbol{k}}$, which ensures the positivity of the excitation energies. This is because the Hamiltonian $H_{\boldsymbol{k}}^\sigma$ under this condition is adiabatically connected to $1_{N\times N}\otimes\sigma_z$ without closing the gap between the particle and hole bands [12]. In the following, we seek another possibility: the boundary states induced by the polarization of the particle (hole) bands.

## III. MODEL WITH NONTRIVIAL BERRY PHASE

According to the "modern theory" of polarization [26], the bulk polarization is given by the Berry phase (divided by $2\pi$) that is defined as the integration of the Berry connection on a noncontractible loop in the Brillouin zone. In one dimension, the Berry phase is given by

$$\gamma_i = i\int_{-\pi}^{\pi} dk\ \langle k, i|\,\partial_k\,|k, i\rangle\,, \tag{12}$$

where $k$ is the one-dimensional crystal momentum with lattice constant $a = 1$. In recent topological physics, bulk polarization is known as another route to induce the boundary states. We here generalize this idea to the particle (hole) bands of a bosonic BdG Hamiltonian.

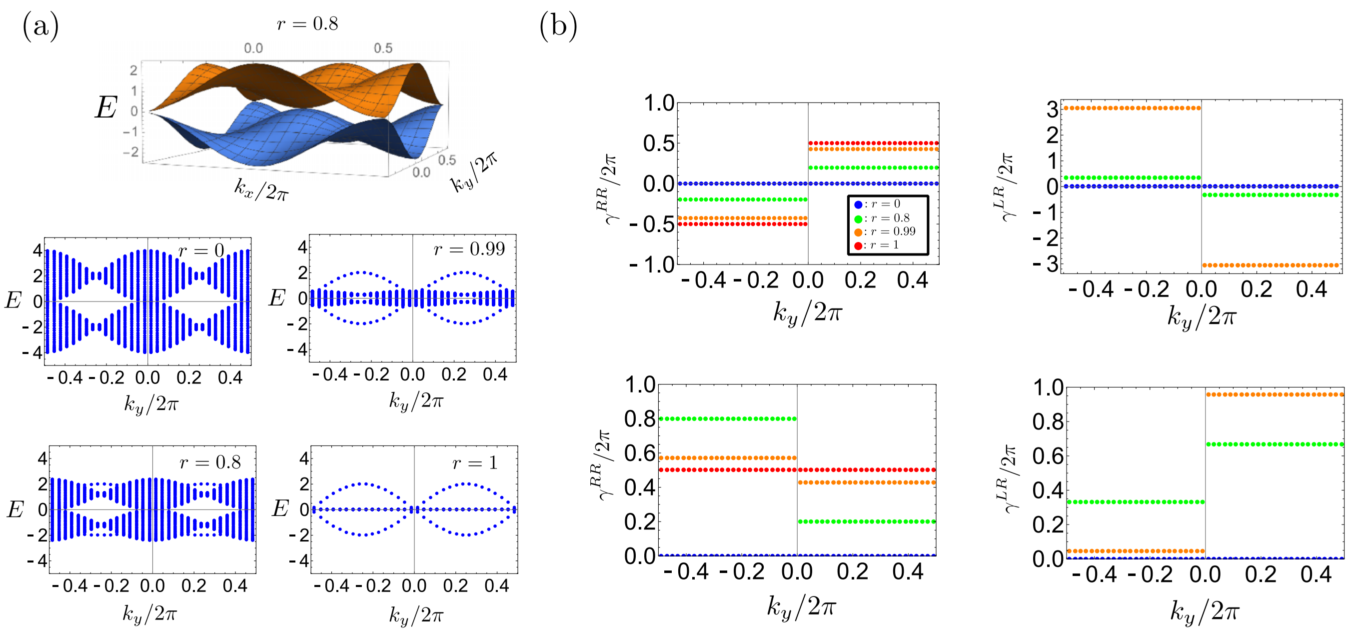


FIG. 1. (a) Band structure for $r = 0.8$ and $k_y$-resolved dispersion on a cylinder (open/periodic boundary condition in the $x/y$ direction) for various $r$. The system size is $32 \times 32$. A $\pi$ flux is inserted in the cylinder to avoid $k_y = 0, \pi$. (b) Berry phases $\gamma^{RR}$ and $\gamma^{LR}$ of the hole band for various $r$. Upper panel: Calculation using a Bloch wave that is a continuous function of $\boldsymbol{k}$. Lower panel: The remainder of the Berry phase divided by $2\pi$. The momenta $k_y = 0, \pi$ are avoided. The system size is $200 \times 50$. For numerical integration, the size in the $x$ direction is taken much larger than that in the $y$ direction.

Let us consider the following two-dimensional bosonic BdG Hamiltonian:

$$H^{\sigma}_{\boldsymbol{k}} = 2t(1 - \cos k_x \cos k_y)\sigma_z + 2i\,t\,r[(\cos k_y - \cos k_x)\sigma_x + \sin k_x \sin k_y \sigma_y], \tag{13}$$

where $r \geqslant 0$ describes the strength of the paring term. In the following, we set the hopping parameter $t$ to unity. This Hamiltonian satisfies Eqs. (4) and (5). The eigenspectrum is calculated as

$$\begin{aligned} E_{\pm}(\boldsymbol{k}) &= \pm 2\sqrt{(1 - \cos k_x \cos k_y)^2 - r^2[(\cos k_y - \cos k_x)^2 + (\sin k_x \sin k_y)^2]} \\ &= \pm 2\sqrt{1 - r^2}(1 - \cos k_x \cos k_y), \end{aligned} \tag{14}$$

where $\pm$ denotes particle and hole bands [Fig. 1(a)]. From this expression, we further assume $r \leqslant 1$ to ensure the nonnegativity of particle energies, $E_{+}(\boldsymbol{k}) \geqslant 0$, which is the condition for the stable ground state. At the extreme limit $r = 1$, the energy spectrum becomes flat. At this limit, $H^{\sigma}_{\boldsymbol{k}}$ is defective except for $k = (0, 0)$ and $(\pi, \pi)$, which physically corresponds to the infinite squeezing limit in the original Hamiltonian (1). Since the particle and hole bands do not experience the band crossing between the $r = 0$ (obviously trivial case) and $r = 1$, one cannot find any conventional topological number such as the Chern number.

The Bloch Hamiltonian (13) describes a system with periodic boundary conditions in both the $x$ and $y$ directions. To discuss the corresponding boundary states, we impose the open/periodic boundary condition in the $x/y$ direction. For a fixed $k_y$, the real-space representation of the Hamiltonian becomes a one-dimensional nearest-neighbor hopping Hamiltonian in the $x$ direction. We define the open boundary by erasing the hopping at the left and right boundaries. In Fig. 1(a), we plot the eigenspectrum with respect to the momentum in the $y$ direction, $k_y$. While there are no isolated modes for $r = 0$, we find the isolated modes outside the bulk particle and hole bands for a large $r$. This behavior is very different from that of Hermitian boundary states, which are located inside the band gap.

In the following, we discuss the physical origin of the out-of-gap boundary modes. The paring term is proportional to an effective model of the quadratic band touching in Hermitian topological physics. In Hermitian physics, the quadratic band touching has been discussed in terms of the geometry-induced surface states [27] and the Euler number [28–30]. In our case, the pairing term has zero-energy boundary modes, which means that the pairing order parameter is broken at the boundary. In the case of fermionic superconductors, the pairing term causes the level repulsion between the particle and hole bands, and the breakdown of the order parameter means the emergence of in-gap states called the Andreev bound states (ABS). In our bosonic case, on the other hand, the pairing term causes the level attraction due to the non-Hermitian aspect, and the breakdown of the order parameter means the emergence of the "out-of-gap" bound states. We call the present bound states at the boundaries the bosonic ABS.

At some $k_y$, the isolated modes are absorbed into the bulk bands. The isolated modes do not degenerate at each momentum $k_y$ and are localized at one boundary. The side of this localization depends on the sign of $k_y$ and the particle-hole band index. At the extreme limit $r = 1$, the low-energy dispersion of the boundary states becomes linear and gapless, and the boundary states are connected to the bulk states at momenta $k_y = 0, \pi$. In other words, the boundary states look like chiral boundary modes around these symmetric points.

These boundary modes are induced by the bulk polarization defined for the Bloch states. In the non-Hermitian (pseudo-Hermitian) cases, however, one can define two types of Berry connections at each momentum $k_y$:

$$\gamma_i^{LR}(k_y) = i\int_{-\pi}^{\pi} dk_x \langle\langle \boldsymbol{k}, i|\partial_{k_x}|\boldsymbol{k}, i\rangle, \tag{15}$$

$$\gamma_i^{RR}(k_y) = i\int_{-\pi}^{\pi} dk_x \langle \boldsymbol{k}, i|\partial_{k_x}|\boldsymbol{k}, i\rangle. \tag{16}$$

The former definition [24,25], which uses both the right and left eigenvectors, reflects the conventional manner in the line-gap topology. In this definition, we have assumed the biorthonormal conventions (9) and (10). The latter definition, which uses only the right eigenvectors, looks like the Hermitian Berry phase. The crucial difference from the Hermitian one is that the set of the right eigenvectors can not span the whole Hilbert space if the paring term is nonzero. In this definition, we have assumed the normalization $\langle \boldsymbol{k}, i|\boldsymbol{k}, i\rangle = 1$. The Berry connections in both definitions take real values under the present biorthonormal/normal conventions. Owing to the gauge degree of freedom, the Berry phases (15) and (16) are determined modulo $2\pi$. In Fig. 1(b), we plot two types of the Berry phases of the hole band at each $k_y$, defined by Eqs. (15) and (16). In the calculation, we have used a Bloch wave that is a continuous function of momentum. The bare values that are not always in $[0, 2\pi)$ are plotted in the upper panel, while the values modulo $2\pi$ are plotted in the lower panel. As $r$ is increased, $\gamma^{RR}$ converges to $\pm\pi$ for positive/negative $k_y$. In Hermitian topological physics, the value $\pi$ indicates the emergence of the boundary states, which indicates that $\gamma^{RR}$ can characterize the observed boundary states. Another definition $\gamma^{LR}$, on the other hand, diverges as for the increase of $r$. Moreover, one cannot define it at the extreme limit $r = 1$ because $\langle \boldsymbol{k}, i|\sigma_z|\boldsymbol{k}, i\rangle = 0$, which leads to the failure of the biorthonormal convention. Thus, we conclude that $\gamma^{RR}$ is the true definition to characterize the present boundary states.

Note that these boundary states are essentially different from the bosonic topological boundary modes in previous studies that are defined for the gap between the particle bands. In our case, the boundary states are characterized by a quantity that is defined for the gap between the particle and hole bands.

### IV. NON-HERMITIAN TOPOLOGY AT FLAT-BAND LIMIT

For general $r$, the bosonic ABS is geometrical rather than topological because the Berry phase $\gamma^{RR}$ varies continuously and is adiabatically connected to zero. At the extreme limit $r = 0$, however, one can find a non-Hermitian topology in the following sense. In this limit, the band becomes completely flat, and its energy is exactly zero. Owing to the particle-hole symmetry, $\sigma_x|-\boldsymbol{k}, i\rangle^*$ is an eigenstate of $H_{\boldsymbol{k}}^{\sigma}$ with an eigenenergy $-\epsilon_{-\boldsymbol{k},i}$. In the present case, both $|\boldsymbol{k}, i\rangle$ and $\sigma_x|-\boldsymbol{k}, i\rangle^*$ are the zero-energy states. Moreover, the Hamiltonian $H_{\boldsymbol{k}}^{\sigma}$ is defective (i.e., not diagonalizable), and the hole eigenstate is identical to the particle one, except for at $\boldsymbol{k} = (0, 0)$ and $(\pi, \pi)$. Thus, $|\boldsymbol{k}, i\rangle$ is identical to $\sigma_x|-\boldsymbol{k}, i\rangle^*$ up to the phase, which means that the particle-hole symmetry effectively acts as if the time-reversal symmetry is at $r = 1$. In addition, $H_{\boldsymbol{k}}^{\sigma}$ is invariant under the inversion $\boldsymbol{k} \to -\boldsymbol{k}$. In total, we can define an effective parity-time symmetry, and $|\boldsymbol{k}, i\rangle$ is identical to $\sigma_x|\boldsymbol{k}, i\rangle^*$ up to the phase. It is known that the Berry phase under this type of antiunitary symmetry is $\mathbb{Z}_2$ quantized [31]. In the present case, it is checked by the following calculation:

$$\begin{aligned}\gamma_i^{RR}(k_y) &\equiv i\int_{-\pi}^{\pi} dk_x \langle \boldsymbol{k}, i|^*\sigma_x\partial_{k_x}\sigma_x|\boldsymbol{k}, i\rangle^* \pmod{2\pi}\\ &= -\gamma_i^{RR}(k_y).\end{aligned} \tag{17}$$

From this relation, the Berry phase is quantized to 0 or $\pi$. The bosonic ABS corresponds to $\gamma_i^{RR} = \pi$.

Thanks to the two-band nature, the above physics is also explained by a $\mathbb{Z}$ topology of the Hamiltonian itself. The Bloch Hamiltonian in the defective region takes the following form:

$$H_{\boldsymbol{k}}^{\sigma} \propto \begin{pmatrix} 1 & ih_{\boldsymbol{k}}^* \\ ih_{\boldsymbol{k}} & -1 \end{pmatrix}, \tag{18}$$

where $h_{\boldsymbol{k}} \in \mathbb{C}$ is on the unit circle in the complex plane. In other words, the degree of freedom of the Bloch Hamiltonian is limited to U(1) if we impose that the matrix is defective. Thus, one can define the winding number on a closed loop $C$ in the Brillouin zone:

$$W = \frac{1}{2\pi i}\oint_C d\ln h. \tag{19}$$

This winding number (19) characterizes two related properties. First, it describes the polarization at each $k_y$:

$$W(k_y) = \frac{1}{2\pi i}\int_{-\pi}^{\pi} dk_x \frac{d\ln h}{dk_x} = \int_{-\pi}^{\pi}\frac{dk_x}{2\pi}\theta_{\boldsymbol{k}}, \tag{20}$$

where $\theta_{\boldsymbol{k}} = \arg(h_{\boldsymbol{k}})$. At special points $k_y = \pm\pi/2$, the winding number is $\pm 1$, which is easily calculated by $\theta_{\boldsymbol{k}} = \pm k_x$. At general $k_y$ except for $k_y = 0, \pi$, $W(k_y) = \mathrm{sgn}(k_y)$. Remarkably, the $\mathbb{Z}$ topological number can distinguish $\pm 1$, while the Berry phase cannot. Second, the winding number (19) detects the nondefective points in the Brillouin zone. Near the nondefective point $\boldsymbol{k} = (0, 0)$, the Hamiltonian takes the following form:

$$\begin{aligned}H_{\boldsymbol{k}}^{\sigma} &\simeq (k_x^2 + k_y^2)\sigma_z + i(k_x^2 - k_y^2)\sigma_x + 2ik_xk_y\sigma_y\\ &\propto \begin{pmatrix} 1 & ie^{-i2\phi} \\ ie^{i2\phi} & -1 \end{pmatrix},\end{aligned} \tag{21}$$

where $\boldsymbol{k} = k(\cos\phi, \sin\phi)$ with $k = |\boldsymbol{k}|$. Thus, $\boldsymbol{k} = (0, 0)$ is characterized by $W = +2$. Similarly, $\boldsymbol{k} = (\pi, \pi)$ is characterized by $W = -2$. The total winding number around nondefective points is zero, which is a non-Hermitian analogy of the Nielsen-Ninomiya theorem [32]. These nondefective points correspond to the quadratic band touching points of the non-Hermitian part of the Hamiltonian, or the pairing term.

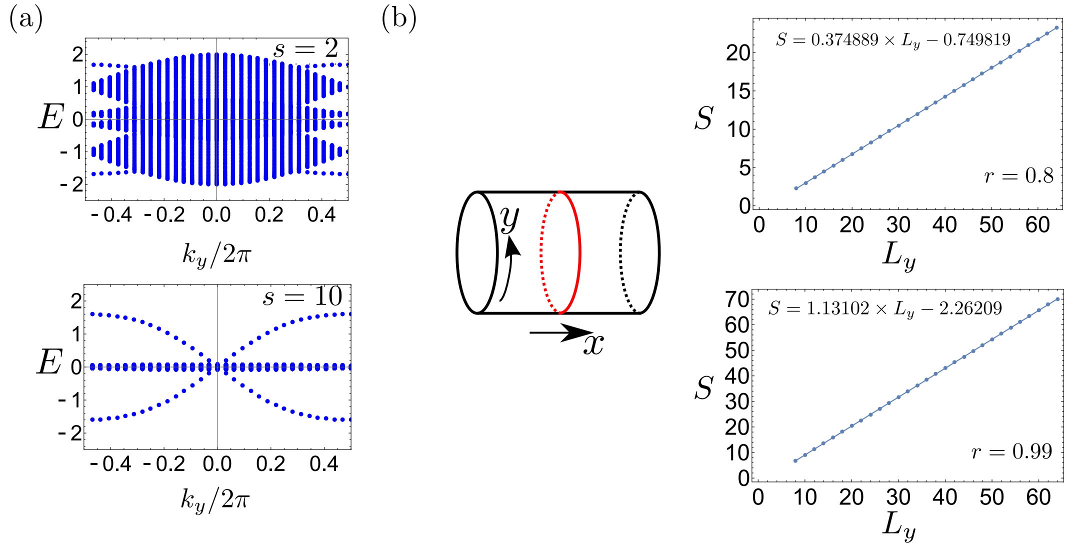


FIG. 2. (a) The Bogoliubov spectrum of the physical CVSC [33] on the cylinder. $s$ is the squeezing parameter. The system size is $32 \times 32$. (b) Size dependence of the entanglement entropy of the ground state of the model (13) on the cylinder.

Note that the above "topological invariant" is not defined for the spectral gap. In the present case, the "gapped" and "gapless" structures correspond to the defective and nondefective structures, respectively.

## V. ENTANGLEMENT ENTROPY OF A MODEL WITH BOSONIC ANDREEV BOUND STATES

Another interesting issue is the entanglement property of the ground state of a model with the bosonic ABS. In free bosonic systems, the entanglement entropy of the ground state is induced only by the paring term. Such a term is naturally introduced by squeezed states of light and plays an important role in continuous-variable (CV) quantum computing [6]. In our calculation [Fig. 2(a)], boundary states similar to those in our model (but with degeneracy) are found in the CV surface codes (CVSC) [33–36]. Reference [33] claims that topological entanglement entropy [37,38] is not quantized in a physical CVSC. In the following, we investigate the entanglement structure of the ground state of the model (13) by using the formula in Ref. [39] and find behaviors similar to those in CVSC. Motivated by these facts, we investigate the entanglement entropy of our model (13). We here investigate the cylindrical configuration ($x$: open, $y$: periodic) and measure the entanglement entropy $S$ of the ground state for half of the system with $L_x = 2L_y$. A formula for the entanglement entropy of the quantum harmonic oscillator, which is identical to the bosonic BdG system, is given in Ref. [39]. Using this formula with the Fourier transform, we calculate the size dependence of the entanglement entropy [Fig. 2(b)]. While the dominant term obeys the area law [i.e., $S_{\rm dom} \propto L_y$], there is a negative constant subleading term. The value depends on the model parameter $r$, which is similar to the behavior of the physical CVSC. In gapped systems, this type of subleading term is called topological entanglement entropy because it characterizes the topological order [37,38]. Unlike in the gapped systems, the constant subleading term is not quantized in the physical CVSC and our model.

## VI. DISCUSSION

We here discuss the bosonic ABS in other dimensions. In one dimension, the realization of a model with one positive- and one negative-energy boundary states localized at opposite boundaries seems to be difficult. If possible, these boundary states are related to each other by the particle-hole symmetry, which does not act on real-space coordinates. Thus, the boundary states are localized at the same boundary, which conflicts with the localization at the opposite boundaries. In our two-dimensional model, the particle-hole symmetry is absent at each $k_y$ except for $0, \pi$, and the localization at the opposite boundary is allowed in each momentum sector. Instead, one can consider the bosonic ABS in a model with a unitary symmetry. For example, let us consider the following one-dimensional model:

$$H_k^\sigma = 1_{2\times 2} \otimes \sigma_z + ir(\cos k\tau_x + \sin k\tau_y) \otimes \sigma_y, \tag{22}$$

where $\tau$'s are the Pauli matrices in orbital space, and $0 \leqslant r \leqslant 1$. This model commutes with $\tau_z \otimes \sigma_z$ and is block diagonalized into $\tau_z \otimes \sigma_z = \pm 1$ sectors. Each block is given by

$$\begin{pmatrix} 1 & ire^{\mp ik} \\ ire^{\pm ik} & -1 \end{pmatrix}, \tag{23}$$

which is the nontrivial polarization. A generalization of the bosonic ABS may be an interesting future work.

## ACKNOWLEDGMENTS

I thank T. Mizoguchi for the fruitful discussions. This work was supported by JSPS KAKENHI Grants No. JP20K14373 and No. JP23K03243.

## APPENDIX: EXPLICIT CONSTRUCTION OF PARAUNITARY MATRIX

We here describe an explicit construction of the paraunitary matrix in Eq. (7). See Ref. [12] for details. The first step is to decompose $H_k$ by the Cholesky decomposition:

$$H_k = K_k^\dagger K_k, \tag{A1}$$

where $K_k$ is an upper triangle matrix. The next step is diagonalization of the Hermitian matrix $W_k := K_k \sigma_z K_k^\dagger$:

$$U_k^\dagger W_k U_k = \begin{pmatrix} E_k & 0 \\ 0 & -E_{-k} \end{pmatrix}, \tag{A2}$$

where $U_k$ is a unitary matrix. The diagonal matrices $E_k$ and $-E_{-k}$ give the particle and hole spectrum, as shown below. By using the above matrices, we construct the following matrix:

$$P_k = K_k^{-1} U_k \begin{pmatrix} E_k^{\frac{1}{2}} & 0 \\ 0 & E_{-k}^{\frac{1}{2}} \end{pmatrix}. \tag{A3}$$

This matrix satisfies the paraunitary condition

$$\begin{aligned} P_k \sigma_z P_k^\dagger &= K_k^{-1} U_k \begin{pmatrix} E_k & 0 \\ 0 & -E_{-k} \end{pmatrix} U_k^\dagger (K_k^{-1})^\dagger \\ &= K_k^{-1} K_k \sigma_z K_k^\dagger (K_k^{-1})^\dagger \\ &= \sigma_z. \end{aligned} \tag{A4}$$

The paraunitary matrix $P_k$ diagonalizes the non-Hermitian bosonic BdG Hamiltonian $H_k^\sigma := \sigma_z H_k$. This can be easily checked:

$$\begin{aligned} &P_k^{-1} \sigma_z H_k P_k \\ &= \begin{pmatrix} E_k^{-\frac{1}{2}} & 0 \\ 0 & E_{-k}^{-\frac{1}{2}} \end{pmatrix} U_k^\dagger K_k \sigma_z K_k^\dagger K_k K_k^{-1} U_k \begin{pmatrix} E_k^{\frac{1}{2}} & 0 \\ 0 & E_{-k}^{\frac{1}{2}} \end{pmatrix} \\ &= \begin{pmatrix} E_k^{-\frac{1}{2}} & 0 \\ 0 & E_{-k}^{-\frac{1}{2}} \end{pmatrix} U_k^\dagger W_k U_k \begin{pmatrix} E_k^{\frac{1}{2}} & 0 \\ 0 & E_{-k}^{\frac{1}{2}} \end{pmatrix} \\ &= \begin{pmatrix} E_k & 0 \\ 0 & -E_{-k} \end{pmatrix}. \end{aligned} \tag{A5}$$


[1] N. Bogoliubov, On the theory of superfluidity, J. Phys. **11**, 23 (1947).
[2] J. Colpa, Diagonalization of the quadratic boson Hamiltonian, Physica A **93**, 327 (1978).
[3] Y. Kawaguchi and M. Ueda, Spinor Bose–Einstein condensates, Phys. Rep. **520**, 253 (2012).
[4] A. Altland and B. D. Simons, *Condensed Matter Field Theory* (Cambridge University Press, Cambridge, 2010).
[5] T. Ozawa, H. M. Price, A. Amo, N. Goldman, M. Hafezi, L. Lu, M. C. Rechtsman, D. Schuster, J. Simon, O. Zilberberg *et al.*, Topological photonics, Rev. Mod. Phys. **91**, 015006 (2019).
[6] S. L. Braunstein and P. V. Loock, Quantum information with continuous variables, Rev. Mod. Phys. **77**, 513 (2005).
[7] P. A. McClarty, Topological magnons: A review, Annu. Rev. Condens. Matter Phys. **13**, 171 (2022).
[8] L. Zhang, J. Ren, J.-S. Wang, and B. Li, Topological nature of the phonon Hall effect, Phys. Rev. Lett. **105**, 225901 (2010).
[9] S. Lieu, Topological symmetry classes for non-Hermitian models and connections to the bosonic Bogoliubov–de Gennes equation, Phys. Rev. B **98**, 115135 (2018).
[10] X.-L. Qi and S.-C. Zhang, Topological insulators and superconductors, Rev. Mod. Phys. **83**, 1057 (2011).
[11] M. Z. Hasan and C. L. Kane, *Colloquium:* Topological insulators, Rev. Mod. Phys. **82**, 3045 (2010).
[12] R. Shindou, R. Matsumoto, S. Murakami, and J.-I. Ohe, Topological chiral magnonic edge mode in a magnonic crystal, Phys. Rev. B **87**, 174427 (2013).
[13] Y. Hatsugai, Chern number and edge states in the integer quantum Hall effect, Phys. Rev. Lett. **71**, 3697 (1993).
[14] H. Kondo, Y. Akagi, and H. Katsura, $\mathbb{Z}_2$ topological invariant for magnon spin Hall systems, Phys. Rev. B **99**, 041110(R) (2019).
[15] Y. Ashida, Z. Gong, and M. Ueda, Non-Hermitian physics, Adv. Phys. **69**, 249 (2020).
[16] N. Okuma and M. Sato, Non-Hermitian topological phenomena: A review, Annu. Rev. Condens. Matter Phys. **14**, 83 (2023).
[17] R. Lin, T. Tai, L. Li, and C. H. Lee, Topological non-Hermitian skin effect, Front. Phys. **18**, 53605 (2023).
[18] K. Kawabata, K. Shiozaki, M. Ueda, and M. Sato, Symmetry and topology in non-Hermitian physics, Phys. Rev. X **9**, 041015 (2019).
[19] Y. Tanaka, M. Sato, and N. Nagaosa, Symmetry and topology in superconductors–odd-frequency pairing and edge states–, J. Phys. Soc. Jpn. **81**, 011013 (2011).
[20] M. Sato and S. Fujimoto, Majorana fermions and topology in superconductors, J. Phys. Soc. Jpn. **85**, 072001 (2016).
[21] A. P. Schnyder, S. Ryu, A. Furusaki, and A. W. W. Ludwig, Classification of topological insulators and superconductors in three spatial dimensions, Phys. Rev. B **78**, 195125 (2008).
[22] A. Kitaev, Periodic table for topological insulators and superconductors, in *AIP Conference Proceedings* (American Institute of Physics, 2009), Vol. 1134, pp. 22–30.
[23] In some isolated cold atomic systems, negative- or complex-energy states are relevant in physics. See Refs. [3,24].
[24] T. Ohashi, S. Kobayashi, and Y. Kawaguchi, Generalized Berry phase for a bosonic Bogoliubov system with exceptional points, Phys. Rev. A **101**, 013625 (2020).
[25] G. Engelhardt and T. Brandes, Topological Bogoliubov excitations in inversion-symmetric systems of interacting bosons, Phys. Rev. A **91**, 053621 (2015).
[26] N. A. Spaldin, A beginner's guide to the modern theory of polarization, J. Solid State Chem. **195**, 2 (2012).
[27] B.-J. Yang and N. Nagaosa, Emergent topological phenomena in thin films of pyrochlore iridates, Phys. Rev. Lett. **112**, 246402 (2014).

[28] J. Ahn, S. Park, and B.-J. Yang, Failure of nielsen-ninomiya theorem and fragile topology in two-dimensional systems with space-time inversion symmetry: Application to twisted bilayer graphene at magic angle, Phys. Rev. X **9**, 021013 (2019).

[29] A. Bouhon, Q. Wu, R.-J. Slager, H. Weng, O. V. Yazyev, and T. Bzdušek, Non-Abelian reciprocal braiding of Weyl points and its manifestation in ZrTe, Nat. Phys. **16**, 1137 (2020).

[30] A. S. Morris, A. Bouhon, and R.-J. Slager, Andreev reflection in Euler materials, New J. Phys. **26**, 023014 (2024).

[31] Y. Hatsugai, Quantized Berry phases as a local order parameter of a quantum liquid, J. Phys. Soc. Jpn. **75**, 123601 (2006).

[32] H. B. Nielsen and M. Ninomiya, No-go theorum for regularizing chiral fermions, Tech. Rep., Science Research Council, 1981.

[33] T. F. Demarie, T. Linjordet, N. C. Menicucci, and G. K. Brennen, Detecting topological entanglement entropy in a lattice of quantum harmonic oscillators, New J. Phys. **16**, 085011 (2014).

[34] J. Zhang, C. Xie, K. Peng, and P. van Loock, Anyon statistics with continuous variables, Phys. Rev. A **78**, 052121 (2008).

[35] D. F. Milne, N. V. Korolkova, and P. van Loock, Universal quantum computation with continuous-variable Abelian anyons, Phys. Rev. A **85**, 052325 (2012).

[36] T. Morimae, Continuous-variable topological codes, Phys. Rev. A **88**, 042311 (2013).

[37] A. Kitaev and J. Preskill, Topological entanglement entropy, Phys. Rev. Lett. **96**, 110404 (2006).

[38] M. Levin and X.-G. Wen, Detecting topological order in a ground state wave function, Phys. Rev. Lett. **96**, 110405 (2006).

[39] T. F. Demarie, Pedagogical introduction to the entropy of entanglement for gaussian states, arXiv:1209.2748.